



## Comparison of the Otto cycle and the Atkinson cycle with an optimized intake cam profile for a turbocharged spark-ignition engine

Arash Mohammadi<sup>1\*</sup>, Mohsen Mohsenirad<sup>2</sup>, Nima Ajami<sup>2</sup>, AmirHossein Parivar<sup>2</sup>, Mohammad Nejat<sup>2</sup>

<sup>1</sup> Faculty of Mechanical Engineering, Shahid Rajaei Teacher Training University, Tehran, Iran

<sup>2</sup> Irankhodro Powertrain Company (IPCo), Tehran, Iran

### ARTICLE INFO

#### Keywords:

Turbocharged Spark-Ignition Engine  
Optimized Cam Profile  
Fuel Economy  
BSFC

### ABSTRACT

This study investigates the performance of a spark-ignition engine featuring an increased effective compression ratio, achieved by implementing the Atkinson cycle through intake cam profile design. A conventional four-stroke, turbocharged spark-ignition engine with a geometric compression ratio of 9.2 and a peak power output of 112 kW served as the baseline. A validated 1D engine simulation model was developed, incorporating in-cylinder pressure calibration based on a turbulent combustion model. Using this model, Atkinson-cycle operation was realized via intake camshaft optimization. Engine performance was evaluated across a wide range of speeds and loads, focusing primarily on brake-specific fuel consumption (BSFC), torque, and overall fuel economy. A comparative analysis was conducted between the baseline engine and the optimized Atkinson-cycle configuration. The results indicate that optimizing the intake valve timing yields an approximate 2–3% reduction in average fuel consumption, achieving a 2.5% overall improvement. These findings demonstrate that implementing the Atkinson cycle via valve timing modifications effectively enhances fuel economy under the investigated operating conditions.



© 2026 Iranian Society of Engine, Tehran, Iran. This article is an open-access article distributed under the terms and conditions of the Creative Commons Attribution Noncommercial 4.0 International (CC BY-NC 4.0 license). (<https://creativecommons.org/licenses/by-nc/4.0/>).

\* Corresponding author

E-mail address: [amohammadi@sru.ac.ir](mailto:amohammadi@sru.ac.ir) (A. Mohammadi)

Received 4 January 2026; Accepted 1 May 2026

E-ISSN: 2345-4121/ISSN: 1735-5214

**Cite this article:** Mohammadi A, Mohsenirad M, Ajami N, Parivar AH, Nejat M. Comparison of the Otto cycle and the Atkinson cycle with an optimized intake cam profile for a turbocharged spark-ignition engine. The Journal of Engine Research. 2026 Feb 20;72(4):50-63. doi: [10.22034/ER.2026.2078266.1120](https://doi.org/10.22034/ER.2026.2078266.1120)

## 1- Introduction

Researchers and automotive manufacturers are increasingly focusing on mitigating environmental challenges and addressing the depletion of global crude oil reserves through the development of hybrid electric vehicles (HEVs) [1]. These vehicles were introduced as a promising approach to reduce fuel consumption and greenhouse gas (GHG) emissions. The transportation sector accounts for approximately 66% of total global oil consumption, of which nearly 50% is consumed by small passenger cars and light-duty trucks [1]. Improvements in fuel economy and reductions in emissions are achieved through technologies such as engine start-stop systems and regenerative braking for energy recuperation [2]. Furthermore, advanced engine technologies, such as the Atkinson-cycle engine [3], contribute significantly to improving fuel efficiency. Therefore, incorporating a fuel-efficient Atkinson-cycle engine into HEVs can further enhance overall vehicle efficiency and reduce GHG emissions. Figure 1 illustrates the progression of CO and CO<sub>2</sub> emission limits over time, beginning with Euro 1 and culminating in the introduction of Euro 6 in January 2020. Following the implementation of the initial emission regulations, the permissible limits for pollutants—particularly carbon monoxide (CO)—were reduced by approximately 63%. From the Euro 4 standard onward, the CO emission limit has remained constant at 1 g/km [3].

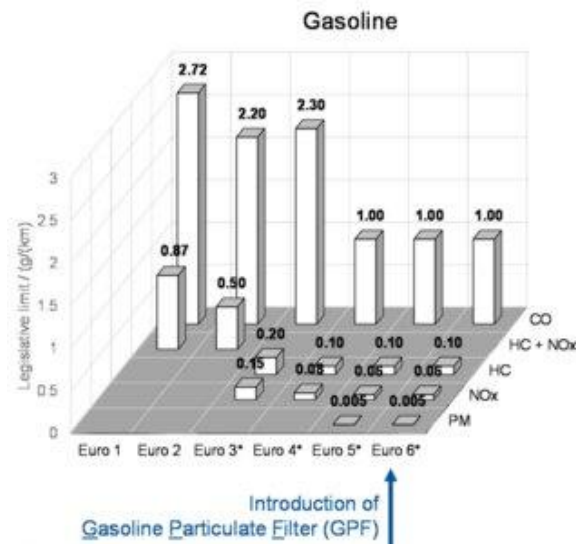


Figure 1 Emission legislation development [3]

James Atkinson, a British engineer, advanced heat engine research in 1882 by designing engines that achieved higher efficiency than the conventional Otto cycle. Today, hybrid electric vehicles (HEVs) increasingly employ Atkinson-cycle engines, which feature a longer expansion stroke and a shorter effective compression stroke. This design enhances thermal efficiency and reduces pollutant emissions. Originating from a patent by Atkinson in 1887, the cycle increases thermal efficiency by allowing over-expansion at the end of the power stroke, effectively decoupling the expansion ratio from the compression ratio. In conventional spark-ignition engines, energy is lost when high-pressure gases are expelled during exhaust valve opening (EVO) instead of being used to perform work on the piston. The Atkinson cycle recovers this residual energy, producing additional work per cycle and thereby increasing indicated work and overall thermal efficiency [4–6] (see Figure 2). However, a limitation of the Atkinson cycle is its strong dependence on engine speed, which can restrict its broader application. Furthermore, because a portion of the intake charge is expelled during the compression stroke, the wide-open throttle (WOT) torque and power output are decreased.

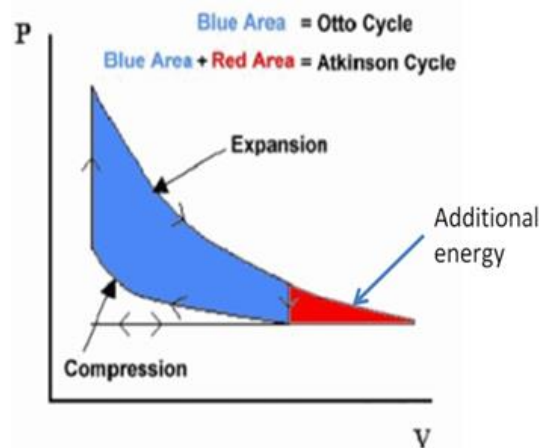


Figure 2 P-V diagram of Atkinson cycle with LIVC mechanism [6]

The Atkinson cycle increases fuel economy by 20–30%, making it an ideal engine type for hybrid electric vehicles (HEVs). According to Qingyu et al. [7], the Atkinson cycle offers an advantage over the Otto cycle in HEVs due to its superior fuel economy. They proposed a performance enhancement strategy by adjusting the compression ratio to optimize cycle efficiency at low-pressure ratios, while increasing the effective compression ratio and modifying the valve closing timing within the constraints of post-compression pressure. Experimental results validated this approach, demonstrating reduced pumping losses, improved fuel economy, and significant gains in cycle efficiency at low to medium pressure ratios. Zhao [8] demonstrated that the over-expansion Atkinson cycle is well-suited for HEVs, as it achieves a high expansion ratio without increasing the risk of engine knock, while simultaneously reducing  $\text{NO}_x$  emissions. The cycle is considered practical for powertrain applications because it lowers exhaust gas temperatures and improves overall thermal efficiency. Yuanhui et al. [9] investigated the engine layout and performance characteristics affecting the Atkinson cycle. They concluded that power is lost due to friction and heat transfer as the compression ratio rises, and that increases in friction loss and cylinder length degrade cycle performance. Shuhn-Shyurng [10] compared the Otto and Atkinson cycles considering heat exchange, clarifying that the work output and thermal efficiency of the Atkinson cycle surpass those of an Otto engine when both are operated under identical conditions [11].

## 2- Atkinson Cycle in HEVs

Recent years have witnessed the widespread adoption of Atkinson-cycle engines in HEVs by major automotive manufacturers, including Toyota, Ford, and Honda. Nearly all HEVs and plug-in hybrid electric vehicles (PHEVs) in the US market—such as the Toyota Prius, Camry Hybrid, Ford Fusion Hybrid, Honda Accord Hybrid, and Chevrolet Volt—are equipped with Atkinson-cycle engines [12]. Technologies such as cooled exhaust gas recirculation (EGR) have been introduced to improve anti-knock capabilities and overall performance. The 2018 Camry Hybrid utilizes Toyota's A25A-FXS engine, a naturally aspirated Atkinson-cycle engine with a compression ratio of 14:1, equipped with variable valve timing (VVT) and cooled EGR. Although detailed specifications of this specific engine are scarce, a similar engine—the A25A-FKS, calibrated for the non-hybrid 2018 Camry—has been extensively studied [13]. It achieves a peak brake thermal efficiency (BTE) of 40%, with  $\text{CO}_2$  emissions reduced by 18.6% compared to the 2015 model year engine, which lacked Atkinson-cycle and EGR features. However, because other improvements were incorporated during the model upgrade, these figures may overstate the isolated contribution of the Atkinson cycle. Similarly, Toyota's 2ZR-FXE engine, used in the third-generation Prius and Lexus CT200h, combines a late intake valve closing (LIVC) Atkinson

cycle, cooled EGR, and port fuel injection (PFI), also achieving a peak BTE of 40%. Beyond manufacturer data, Li et al. investigated the fuel-saving potential of an Atkinson-cycle gasoline engine in a series HEV [13]. Cumulative fuel consumption was reduced by 4.58% compared to the original Otto engine, while NO<sub>x</sub> and CO<sub>2</sub> emissions decreased by 46.1% and 18.37%, respectively. According to EPA predictions, adopting the Atkinson cycle can reduce CO<sub>2</sub> emissions by 3–8% when the effects of EGR and a high compression ratio are included. However, recent progress in engine technologies suggests this benefit could be higher, reaching 10–14% [13]. Furthermore, fuel savings from the Atkinson cycle are projected by agencies to range between 8% and 10.3%, and manufacturers are on track to meet or exceed these figures. It is also estimated that 20–30% of the overall fuel economy improvement in HEVs is directly attributable to the Atkinson cycle [14].

This paper investigates the testing of a parallel HEV equipped with fuel-efficient innovations, specifically an Atkinson-cycle engine. Another vital factor in improving the efficiency of HEV powertrains is the design of advanced energy management control (EMC) strategies to maximize fuel economy benefits.

### 3- Optimization Approach

Multiple operating conditions were analyzed through 1D computational fluid dynamics (CFD) calculations. Various valve lift profiles were simulated to provide additional insights into the impact of Atkinson strategies on factors such as mixture preparation, injection-air interaction, turbulence levels, and auto-ignition. The GT-Power tool was used to conduct these 1D CFD computations [11]. For the Atkinson-cycle engine, four primary optimization variables were initially considered: intake valve opening (IVO) timing, intake valve opening duration (calculated as IVC–IVO), maximum intake valve lift, and EGR rate. The chromosome of each individual can be represented as a vector of real values, where each value corresponds to a specific operating variable (gene). Therefore, each individual in the population represents a unique combination of operating variables for a specific engine speed and torque. The fuel efficiency of each candidate solution (individual) is assessed using a fitness function. Through crossover and mutation operations, new offspring are generated from selected parent individuals within the reproduction pool. With each successive generation, the individuals progressively converge toward the optimal solution, which is characterized by the lowest fitness value.

#### 3-1- Coupling Methodology Between MATLAB-GA, Simulink, and GT-Power

The optimization framework developed in this study integrates a genetic algorithm (GA) implemented in MATLAB, a dynamic system model built in Simulink, and a high-fidelity engine model developed in GT-Power. These three environments are coupled within an automated co-simulation loop to enable model-based engine parameter optimization. The architecture follows a hierarchical master–slave configuration:

- (1) MATLAB (GA) acts as the supervisory optimization layer.
- (2) Simulink functions as the system-level integration and control platform.
- (3) GT-Power operates as the high-fidelity, physics-based engine simulation module.

Coupling is realized through a bidirectional data exchange mechanism, allowing for iterative parameter updates and performance feedback during each optimization generation. The MATLAB-based GA serves as the master controller for the optimization process. The algorithm initializes a population of candidate solutions representing engine design or control parameters. Consequently, a vector  $x = (IVO, IVC, EVC, MAX_{LIFT}, EGR)$  is defined to represent the chromosome of an individual in the population, meaning each chromosome consists of five distinct genes. Optimizations of the operating variables were performed under the same speed–load operating points shown in Figure 2. The GA-based optimization scheme for maximizing fuel economy at a given load point can be depicted as follows:

$$\begin{aligned}
 &\text{Minimize: BSFC} \\
 &\text{Subject to: } 6 \% \leq \text{EGR} \leq 24 \% \\
 &99\% (\text{Max Lift})_{\text{Base}} \leq \text{Max Lift} \leq 101\% (\text{Max Lift})_{\text{Base}} \\
 &80\%(\text{IVC-IVO})_{\text{base}} \leq (\text{IVC-IVO}) \leq 120\%(\text{IVC-IVO})_{\text{base}} \\
 &-30 \text{ ATDC} \leq \text{IVO} \leq 40 \text{ ATDC}
 \end{aligned}$$

For each individual parameter MATLAB transfers the parameter set to the Simulink model via workspace variables. The objective function is formulated as: the fitness function for the GA based fuel economy optimization may be written as:

$$F(x) = BSFC(x) + R \left( \sum_{i=1}^4 \max(\bar{g}_i, 0) + |\bar{h}(x)| \right) \tag{1}$$

After receiving the simulation outputs, the GA performs selection, crossover, and mutation operations to generate a new population. This procedure continues until the convergence criteria (e.g., maximum number of generations or fitness tolerance) are met. The automated, coupled optimization loop proceeds as follows:

1. The GA generates a candidate parameter set.
2. The parameters are written to the MATLAB workspace.
3. The Simulink model is executed programmatically.
4. GT-Power performs the engine simulation within the co-simulation environment.
5. The performance results are returned to MATLAB.
6. The objective function is evaluated.
7. The GA updates the population.

This automated loop eliminates the need for manual intervention and enables the efficient exploration of a high-dimensional parameter space. Figure 3 illustrates the coupling scheme among the MATLAB (GA) program, the Simulink model, and the GT-Power model. The key GA parameters are defined as follows:

- Population size: 50
- Number of generations: 300
- Crossover probability: 0.8 (GT-Power default)
- Mutation probability: 0.01 (GT-Power default)

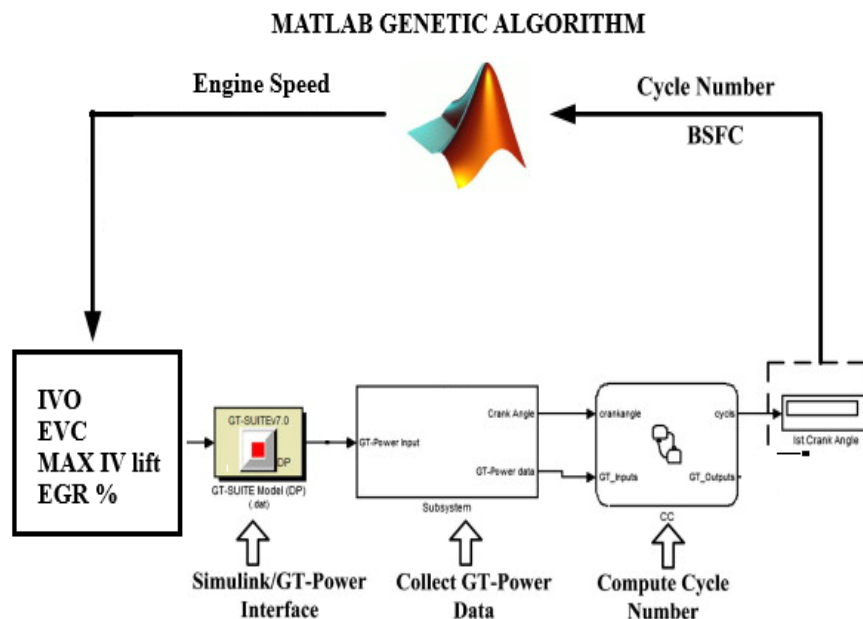


Figure 3 Coupling scheme among the MATLAB (GA) program, Simulink model and GT-Power model

### 3-2- Simulation Model

Figures 4–7 present the optimization results for the engine operating variables at a speed of 2000 rpm and a load of 2 bar, utilizing the GA. Under the defined constraints—intake valve opening (IVO), intake valve closing (IVC), exhaust valve closing (EVC), maximum valve lift, and exhaust gas recirculation (EGR)—all parameters successfully converged to their optimal values. The corresponding optimal brake specific energy consumption (BSEC) was reduced to 333 g/kWh, representing a 3.36% improvement compared to the baseline conditions prior to optimization. Notably, based on the convergence trends of the best fitness value among individuals and the mean fitness of the population, the optimization process terminated before reaching the predefined limit of 370 generations. This early termination occurred because a stopping criterion was implemented in the MATLAB-based GA program: if the best fitness value remains unchanged for 10 consecutive generations, the population is considered to have sufficiently converged. At this point, the algorithm automatically halts to prevent unnecessary computational effort.

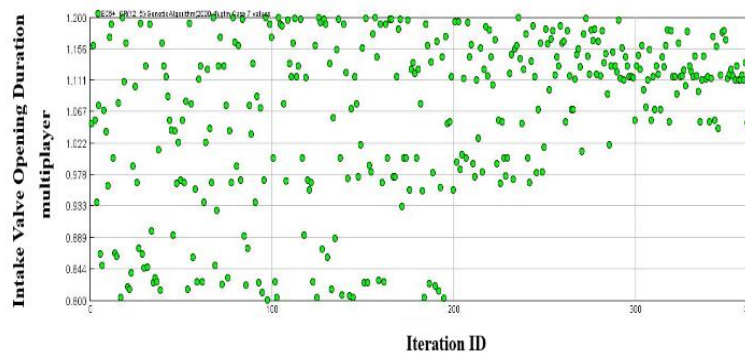


Figure 4 Intake valve opening multiplayer vs. iteration

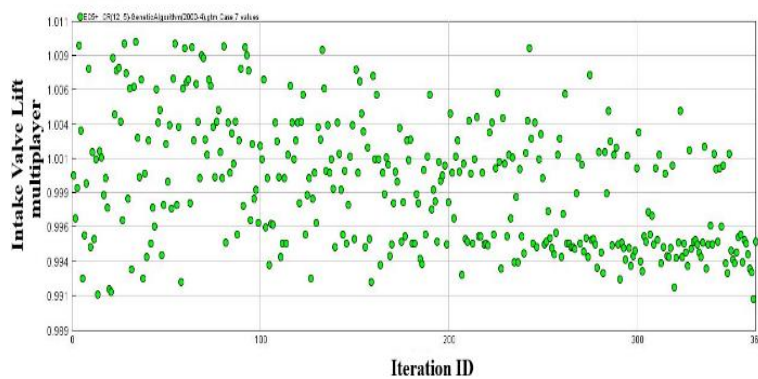


Figure 5 Intake valve lift multiplayer vs. iteration

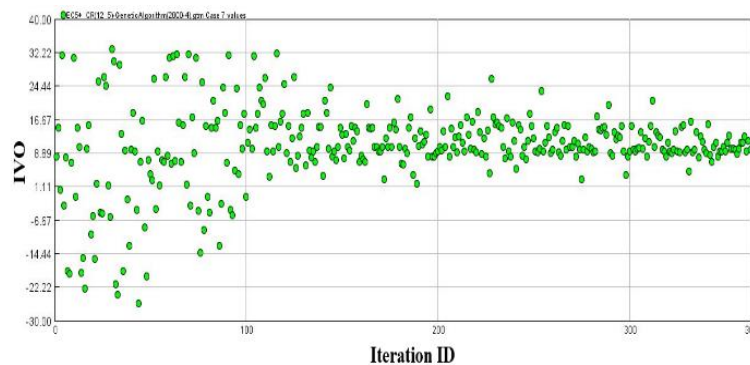


Figure 6 Intake valve opening vs. iteration

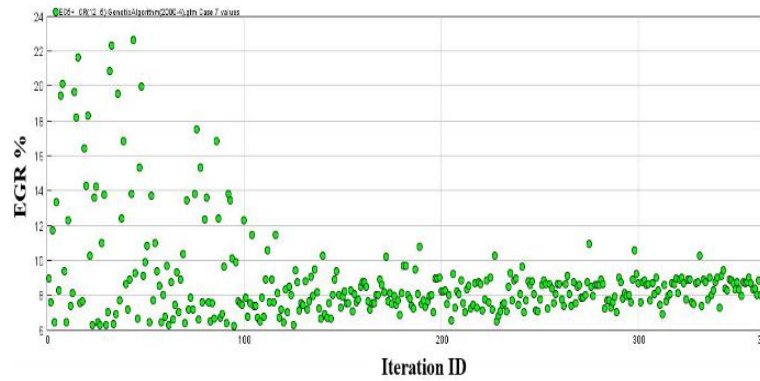


Figure 7 EGR vs. iteration

### 3-3- Validation of numerical 1D modeling

Figure 8 shows comparison of numerical of experimental and 1D numerical data of pressure profile at 2000 rpm and load 2 bar. Results clarify accuracy of numerical results.

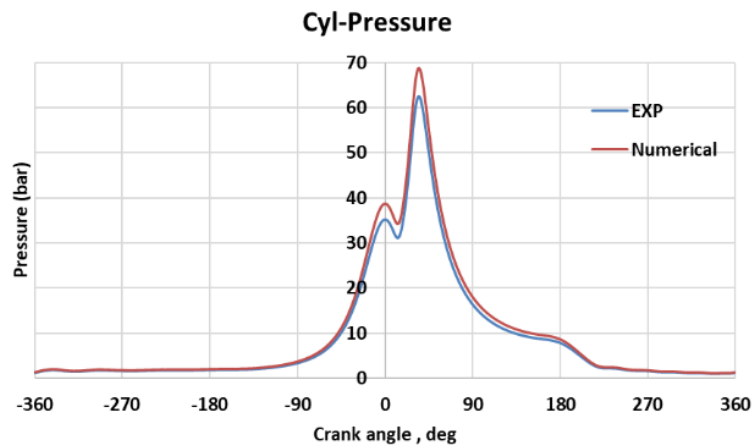


Figure 8 Comparison of numerical of experimental and 1D numerical data of pressure profile

### 3-4- Experimental Setup

The old and new pistons are shown in Figure 9. The pistons were CNC-milled from forgings close to their final shape. As illustrated in Figure 4, two piston head designs were tested: a conventional flat head with a low compression ratio (CR) of 9.5:1, and a deep-bowl design with a high CR of 12:1. Figure 10 presents the optimized intake valve profile obtained using a genetic algorithm.



Figure 9 Piston CR 9.5:1 (left) and piston CR 12:1 (right)

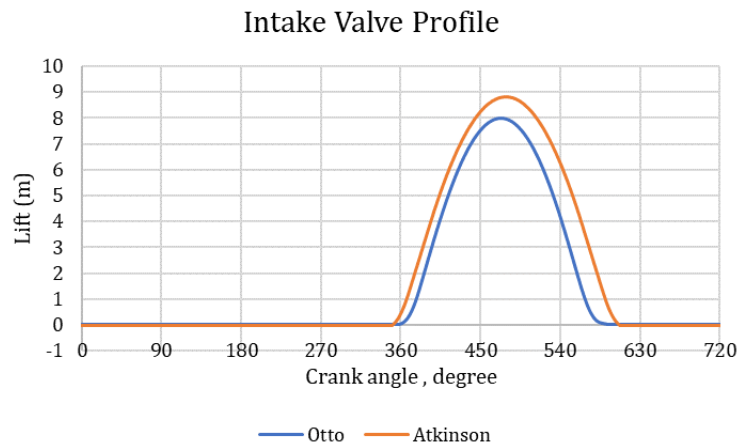


**Figure 10** Optimized intake valve profile with Genetic algorithm

Figure 11 shows a schematic of the 1.6 L, four-cylinder turbocharged gasoline engine studied in this work. The diagram highlights the main functional components, including the air filter, throttle, intake manifold, four cylinders, exhaust manifold, and three-way catalyst (TWC). For brevity, other components such as the crankshaft, camshafts, and pistons are not shown. The Atkinson-cycle engine is a port fuel-injection (PFI) gasoline engine. Fuel consumption is measured using an FC2210Z intelligent fuel consumption meter with an accuracy of  $\pm 0.5\%$ . The engine is coupled to a DYNAS3 LI 250 high-dynamic electric dynamometer, which records engine speed, oil temperature, coolant temperature, and intake air temperature automatically via its control console. Cylinder pressure is measured with a Kistler 6117B pressure sensor integrated with the spark plug, accurate to  $\pm 1.25$  bar, while a Kistler 2613B crank angle encoder (not shown) mounted at the free end of the crankshaft provides crank angle measurements with an accuracy of  $\pm 0.1^\circ$  CA. Both cylinder pressure and crank angle are monitored and recorded by the electronic control unit (ECU). A high-speed data acquisition system (AVL621 combustion analyzer) collects data from the fuel consumption meter, dynamometer, and ECU. The system also incorporates a Horiba MEXA-730L tester, with an accuracy of  $\pm 0.1$ , used to control the air-fuel ratio. The fuel used in this study was pure gasoline with no blends. Table 1 presents the basic specifications of the original Otto-cycle engine.

**Table 1** Original Otto cycle engine basic specifications

Type	Inline, water cooled
Number of cylinders	4
Bore (m)	0.0785
Engine speed (rpm)	1000-3500 rpm
Stroke (mm)	0.082
Connecting rod length(mm)	0.1335
Compression ratio	9.5-12
Diameter on intake valve	3 cm
Diameter on exhaust valve	2.4 cm
Maximum torque/Speed	230 Nm/2500 rpm
Rated power/Speed	112 kW/6000 rpm
Intake valve opening timing	365
Exhaust valve opening timing	156

All experimental measurements were conducted after the engine had warmed up at idle and reached steady-state conditions, with the oil temperature between  $65^\circ\text{C}$  and  $90^\circ\text{C}$ , and the coolant temperature between  $65^\circ\text{C}$  and  $80^\circ\text{C}$ . During the experiments, the oil

temperature was maintained below 135°C, the coolant outlet temperature was controlled within the range of 65–88°C, and the exhaust temperature was kept below 850°C. The engine, as installed on the test rig, is shown in Figure 12.

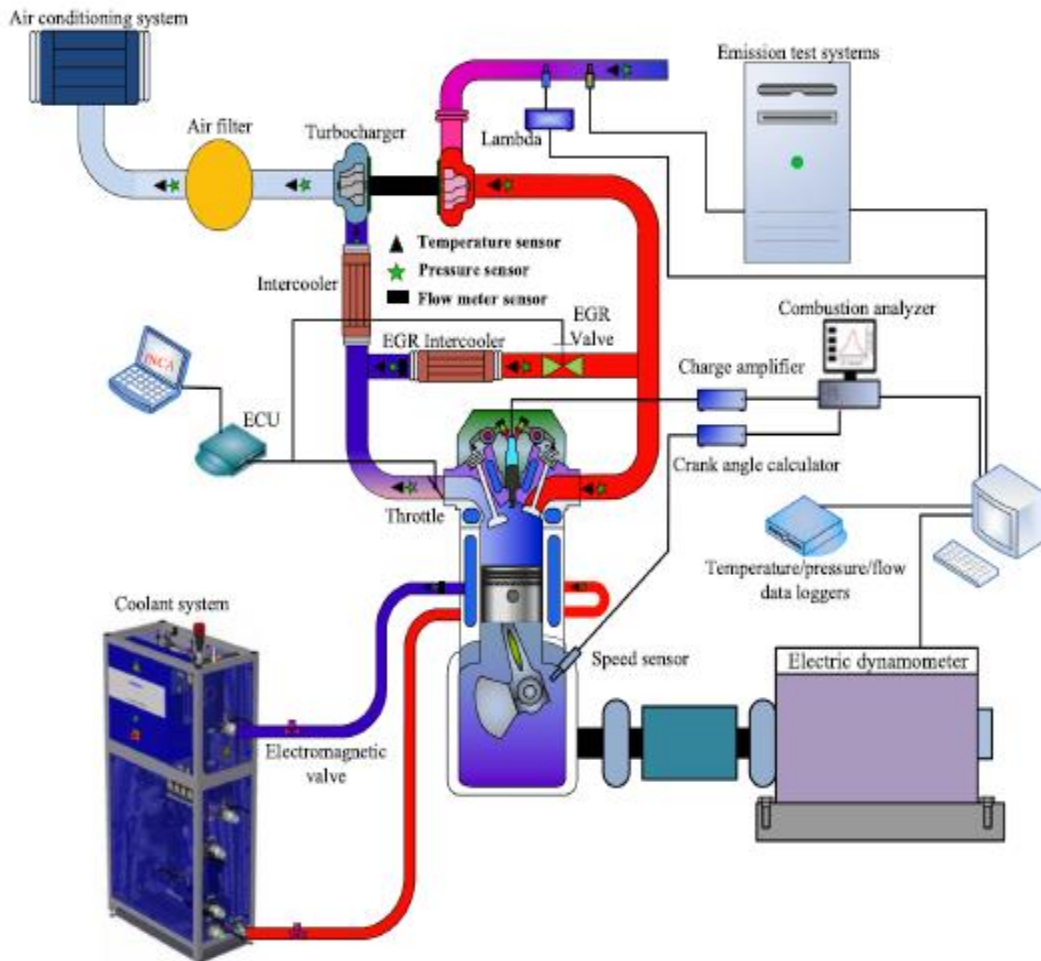


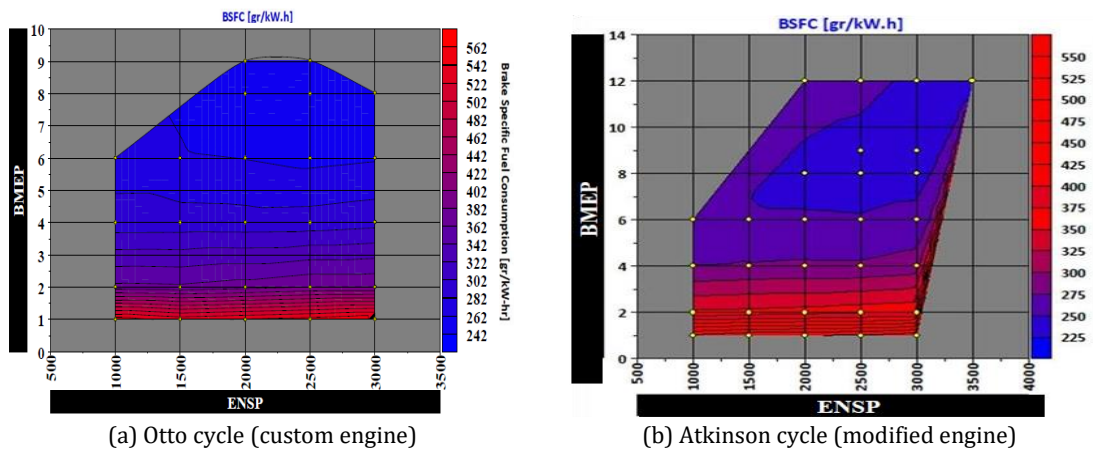
Figure 11 Schematic setup of the Atkinson cycle engine



Figure 12 Engine in the test rig

**4- Results and Discussion**

Figure 13 illustrates the BSFC improvement across the entire engine speed-load range. Here, the improvement is defined as the relative difference between the Otto-cycle BSFC and the GA-optimized Atkinson-cycle BSFC, normalized by the Otto-cycle BSFC. The results demonstrate a clear reduction in fuel consumption for the Atkinson-cycle engine following optimization. These improvements are particularly significant at low loads, as well as at high loads under high-speed conditions. The maximum BSFC reduction occurs at low loads, specifically around 1–2 bar and 2000–3000 rpm. Figure 9 presents the BSFC contour plots for both the Otto- and Atkinson-cycle engines (panels a and b). The area corresponding to 242 g/kWh for the Atkinson-cycle engine is substantially larger than that of the Otto-cycle engine. Additionally, the areas corresponding to 242–302 g/kWh are more extensive for the Atkinson cycle, indicating superior fuel economy in the medium-to-high load range. When utilized in a hybrid vehicle, the Atkinson-cycle engine can achieve significant fuel economy improvements if an appropriate engine operating strategy is adopted. By coordinating the engine and electric motor to operate in their most efficient regions, no-load operation is minimized, and the engine operates primarily in regions characterized by lower fuel consumption. Consequently, HEVs equipped with Atkinson-cycle engines can achieve higher overall fuel efficiency compared to conventional vehicles using Otto-cycle engines. The maps of fuel consumption and torque under different loads at 1000–3500 rpm are shown in Figures 14 and 15.



**Figure 13** BSFC Map of turbocharged engine

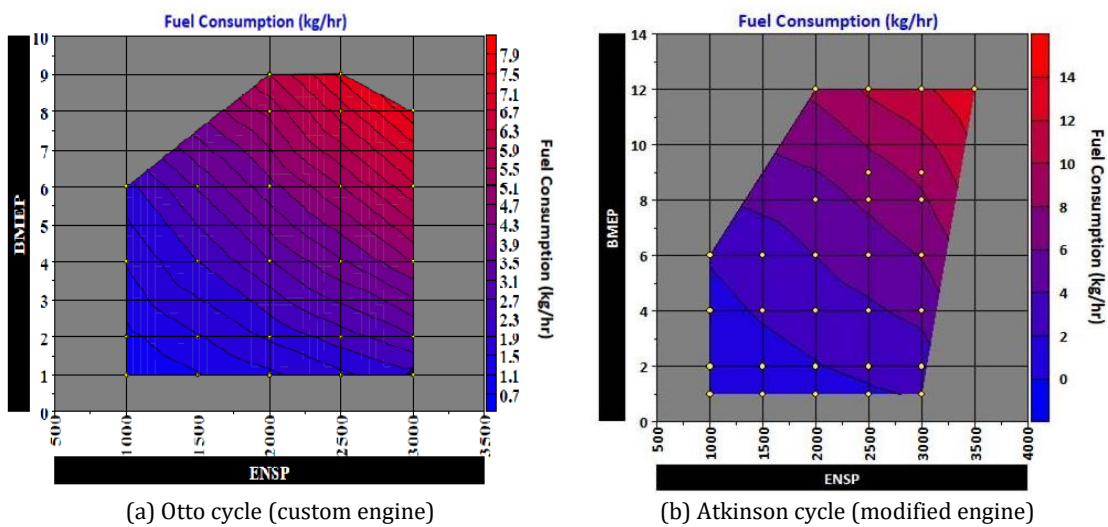


**Figure 14** Fuel Consumption Map of turbocharged engine

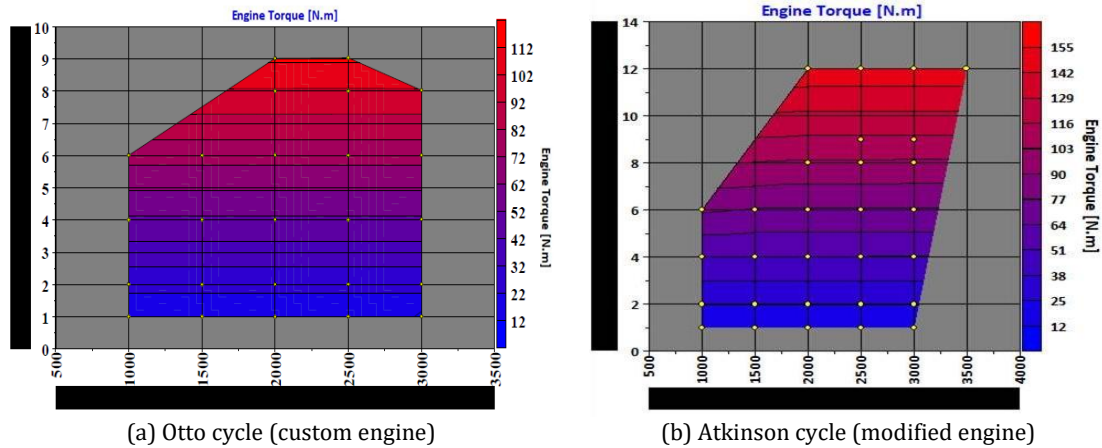


Figure 15 Torque Map of turbocharged engine

The following conclusions are drawn:

- a. Optimization reduces the average fuel consumption rate by 2–3%. At 3000 rpm and 1 bar, the minimum BSFC is 238 g/kWh, while the maximum BSFC at the same operating point is 545 g/kWh.
- b. The absolute fuel consumption rate also decreases by 2–3% after optimization. At 3000 rpm and 1 bar, the minimum fuel consumption is 0.7 kg/h, and the maximum is 13.7 kg/h, as shown in Figure 10.
- c. Engine torque ranges from a minimum of 12.6 N.m at 3000 rpm and 1 bar to a maximum of 151.6 N.m at 3500 rpm and 12 bar, as illustrated in Figure 11.

Table 2 presents a comparison with previously published literature, summarizing the objective functions, methodologies, and key findings.

Table 2 Comparison with prior work in results

Ref	Author (Year)	Engine / Model	Objective	Methodology / Tools	Key Findings
2	Smith et al. (2018)	Turbocharged SI engine	Effect of Atkinson vs Otto on economy	GT-Power simulations	Atkinson improved BSFC up to 4% at part load
4	Lee & Kim (2019)	SI engine with variable valve timing	Intake cam optimization to reduce pumping losses	1D engine model + GA	Optimized intake lift reduced BSFC by 3.2%
5	Gupta & Rao (2020)	Atkinson cycle engine	Performance & emissions comparison	Experimental + simulation	Atkinson had lower NO <sub>x</sub> , slightly lower power
6	Wang et al. (2021)	Miller cycle SI turbo engine	Valve timing effect on BSFC	GT-Power / Simulink co-simulation	Late intake closing reduced BSFC in mid range
8	Zhang & Liu (2021)	Turbocharged SI engine	Multi-objective optimization (BSFC & torque)	NSGA-II + GT-Power	Found Pareto curves for BSFC vs torque
10	Perez et al. (2022)	SI engine with EGR	Intake cam profile design	1D engine model + CFD calibration	Increased EGR reduced pumping losses
13	Singh & Sharma (2023)	Otto vs Atkinson comparison	Cycle performance under load	Simulation + bench measurement	Atkinson better at low to mid load, similar peak power
14	Chen & Huang (2024)	Variable cam engine	Valve timing optimization	Genetic Algorithm + GT-Power	Optimized cam improved economy by 2–3%
15	Oliveira et al. (2024)	SI Turbo engine with Miller	Multi-objective optimization	GT-Power + Pareto optimization	BSFC reduced 3–5%, trade-off with torque

## 5- Challenges, Recommendations, and Future Prospects of the Atkinson Cycle

**Challenges:** The primary limitation of Atkinson-cycle engines is their reduced power density due to intake charge backflow. Although electric motors in hybrid powertrains can compensate for peak power deficits at high loads, achieving higher engine power density remains desirable, as it allows for engine downsizing and further fuel economy improvements.

**Recommendations:** One approach is to combine Otto- and Atkinson-cycle operations within a single engine, utilizing the Otto cycle at high loads and the Atkinson cycle at low-to-medium loads. This strategy increases power density at high loads—albeit with a potential increase in the risk of engine knock—while Atkinson operation improves fuel efficiency via valve timing adjustments [19]. Another solution is to implement the Atkinson cycle in conjunction with turbocharging (i.e., the turbocharged Miller cycle), where boosted intake pressure compensates for the charge loss caused by backflow.

**Future Prospects:** Future research should focus on two primary directions: (1) developing technical strategies to suppress engine knock, thereby enabling safe Otto-cycle operation at high loads within a dual Otto–Atkinson cycle, and (2) designing high-efficiency turbochargers with elevated pressure ratios to meet the intake boost requirements of Atkinson-cycle operation.

## 6- Conclusions and Recommendations for Further Research

In this study, a comprehensive investigation was conducted to optimize the performance of an Atkinson-cycle gasoline engine and assess its fuel-saving potential in series hybrid electric vehicles (HEVs). First, experimental investigations were performed, and a corresponding one-dimensional GT-Power simulation model was developed and validated for a baseline Otto-cycle engine. The model was subsequently modified to represent an Atkinson-cycle engine by adjusting the intake valve timing, intake valve duration, maximum intake valve lift, and exhaust gas recirculation (EGR) settings. Finally, the optimized performance maps were implemented in the simulation of a series HEV equipped with the proposed Atkinson-cycle engine.

## Acknowledgments

The authors would like to express their gratitude to IPCO for their financial support and for providing the experimental test rig.

## References

- [1] Zhao J, Xu M, Li M, Wang B, Liu S. Design and optimization of an Atkinson cycle engine with the Artificial Neural Network Method. *Applied energy*. 2012;92:492–502.
- [2] Zhao J, Li Y, Xu F. The effects of the engine design and operation parameters on the performance of an Atkinson engine considering heat-transfer, friction, combustion efficiency and variable specific-heat. *Energy Conversion and Management*. 2017 Nov 1;151:11-22. doi: [10.1016/j.enconman.2017.08.066](https://doi.org/10.1016/j.enconman.2017.08.066)
- [3] Zhao J. Research and application of over-expansion cycle (Atkinson and Miller) engines—A review. *Applied Energy*. 2017 Jan 1;185:300-19. doi: [10.1016/j.apenergy.2016.10.063](https://doi.org/10.1016/j.apenergy.2016.10.063)
- [4] Yang Z, Narasimhamurthy NM, Miller T, Naber J. Investigation and optimization of cam actuation of an over-expanded atkinson cycle spark-ignited engine. *SAE International Journal of Advances and Current Practices in Mobility*. 2019 Apr 2;1(2019-01-0250):639-53.
- [5] Wang Y, Biswas A, Rodriguez R, Keshavarz-Motamed Z, Emadi A. Hybrid electric vehicle specific engines: State-of-the-art review. *Energy Reports*. 2022 Nov 1;8:832-51. doi: [10.1016/j.egy.2021.11.265](https://doi.org/10.1016/j.egy.2021.11.265)
- [6] Takahashi D, Nakata K, Yoshihara Y, Ohta Y, Nishiura H. Combustion development to achieve engine thermal efficiency of 40% for hybrid vehicles. *SAE Technical Paper*; 2015 Apr 14.

- [7] Niu Q, Sun B, Zhang D, Luo Q. Research on performance optimization and fuel-saving mechanism of an Atkinson cycle gasoline engine at low speed and part load. *Fuel*. 2020 Apr 1;265:117010. doi: [10.1016/j.fuel.2020.117010](https://doi.org/10.1016/j.fuel.2020.117010)
- [8] Niu Q, Sun B, Wu Y, Bao L, Luo Q. Effects of intake valve opening duration on performance optimization of an Atkinson cycle engine under part load. *Proceedings of the Institution of Mechanical Engineers, Part D: Journal of Automobile Engineering*. 2021 Dec;235(14):3557-70.
- [9] Lutsey N, Meszler D, Isenstadt A, German J, Miller J. Efficiency technology and cost assessment for US 2025–2030 light-duty vehicles. International Council on Clean Transportation (ICCT), Washington, USA, White Paper, 22nd March. 2017 Mar 15;45.
- [10] Li Y, Wang S, Duan X, Liu S, Liu J, Hu S. Multi-objective energy management for Atkinson cycle engine and series hybrid electric vehicle based on evolutionary NSGA-II algorithm using digital twins. *Energy Conversion and Management*. 2021 Feb 15;230:113788. doi: [10.1016/j.enconman.2020.113788](https://doi.org/10.1016/j.enconman.2020.113788)
- [11] Li X, Song J, Yu G, Liang Y, Tian H, Shu G, Markides CN. Organic Rankine cycle systems for engine waste-heat recovery: Heat exchanger design in space-constrained applications. *Energy conversion and management*. 2019 Nov 1;199:111968. doi: [10.1016/j.enconman.2019.111968](https://doi.org/10.1016/j.enconman.2019.111968)
- [12] Li J, Yang Z, Hu S, Yang F, Duan Y. Effects of shell-and-tube heat exchanger arranged forms on the thermo-economic performance of organic Rankine cycle systems using hydrocarbons. *Energy Conversion and Management*. 2020 Jan 1;203:112248. doi: [10.1016/j.enconman.2019.112248](https://doi.org/10.1016/j.enconman.2019.112248)
- [13] Cordier M, Laget O, Duffour F, Gautrot X, De Francqueville L. Increasing modern spark ignition engine efficiency: a comprehension study of high CR and Atkinson cycle. InSAE 2016 International Powertrains, Fuels & Lubricants Meeting 2016 Oct 17. SAE Technical Paper.
- [14] Asghar M, Bhatti AI, Ahmed Q, Murtaza G. Energy management strategy for Atkinson cycle engine based parallel hybrid electric vehicle. *IEEE Access*. 2018 May 15;6:28008-18.

## مقایسه عملکرد چرخه اتو و اتکینسون با طرح بادامک بهینه شده در یک موتور اشتعال جرقه‌ای پرخوران

آرش محمدی<sup>۱\*</sup>، محسن محسنی راد<sup>۲</sup>، نیما عجمی<sup>۲</sup>، امیر حسین پریور<sup>۲</sup>، محمد نجات<sup>۲</sup>

<sup>۱</sup> دانشکده مهندسی مکانیک، دانشگاه تربیت دبیر شهید رجایی، تهران، ایران

<sup>۲</sup> شرکت تحقیق، طراحی و تولید موتور ایران خودرو (ایپکو)، تهران، ایران

### چکیده

در این تحقیق، یک موتور احتراق جرقه‌ای با افزایش نسبت تراکم از طریق آزمون موتور با چرخه اتکینسون با طراحی شکل بادامک هوای ورودی بررسی شد. یک موتور پرخوران اشتعال جرقه‌ای چهار زمانه معمولی با نسبت تراکم ۹.۲ و حداکثر توان ۱۱۲ کیلووات برای موتور پایه انتخاب شد. پس از یک الگوی شبیه‌سازی موتور یک بعدی معتبر که شامل تنظیم فشار داخل استوانه با طرح احتراق آشفته موتور اشتعال جرقه‌ای بود، بررسی‌های موتور اتکینسون از جمله بهینه‌سازی میل بادامک ورودی انجام شد. طیف کاملی از سرعت و جابجایی بار برای مقایسه مصرف سوخت ویژه ترمزی انجام شد، مصرف سوخت و گشتاور بین موتور پایه و موتور چرخه اتکینسون با بهینه‌سازی زمان‌بندی دریچه نیز بررسی شد. نتایج حاصل از این مطالعه نشان می‌دهد که میانگین نرخ مصرف سوخت پس از بهینه‌سازی ۲-۳ درصد کاهش می‌یابد، نرخ کاهش مصرف سوخت ۲.۵ درصد است که نشان می‌دهد اقتصاد سوخت در این شرایط عملیاتی بهبود یافته است.

### اطلاعات مقاله

#### کلیدواژه‌ها:

موتور اشتعال جرقه‌ای پرخوران  
بهینه‌سازی شکل میل بادامک  
مصرف سوخت  
مصرف سوخت ویژه ترمزی



© 2026 Iranian Society of Engine, Tehran, Iran. This article is an open-access article distributed under the terms and conditions of the Creative Commons Attribution Noncommercial 4.0 International (CC BY-NC 4.0 license). (<https://creativecommons.org/licenses/by-nc/4.0/>).

\* نویسنده مسئول

پست الکترونیکی: [amohammadi@sru.ac.ir](mailto:amohammadi@sru.ac.ir) (آرش محمدی)

دریافت ۱۴ دی ۱۴۰۴؛ پذیرش ۱۱ اردیبهشت ۱۴۰۵  
شاپای الکترونیکی: ۴۱۲۱-۲۳۴۵ / شاپای چاپی: ۵۲۱۴-۱۷۳۵

**Cite this article:** Mohammadi A, Mohsenirad M, Ajami N, Parivar AH, Nejat M. Comparison of the Otto cycle and the Atkinson cycle with an optimized intake cam profile for a turbocharged spark-ignition engine. The Journal of Engine Research. 2026 Feb 20;72(4):50-63. doi: 10.22034/ER.2026.2078266.1120